

## OPTIMIZATION OF PIN FIN HEAT SINK BY APPLICATION OF CFD SIMULATIONS AND DOE METHODOLOGY WITH NEURAL NETWORK APPROXIMATION

K. KASZA\*

ABB Corporate Research  
ul. Starowińska 13a, 31-038 Kraków, POLAND  
E-mail: krzysztof.kasza@pl.abb.com

Ł. MALINOWSKI

ABB Corporate Research  
ul. Starowińska 13a, 31-038 Kraków, POLAND

I. KRÓLIKOWSKI

AGH University of Science and Technology  
ul. Mickiewicza 30, 30-590 Kraków, POLAND

A design optimization of a staggered pin fin heat sink made of a thermally conductive polymer is presented. The influence of several design parameters like the pin fin height, the diameter, or the number of pins on thermal efficiency of the natural convection heat sink is studied. A limited number of representative heat sink designs were selected by application of the design of experiments (DOE) methodology and their thermal efficiency was evaluated by application of the antecedently validated and verified numerical model. The obtained results were utilized for the development of a response surface and a typical polynomial model was replaced with a neural network approximation. The particle swarm optimization (PSO) algorithm was applied for the neural network training providing very accurate characterization of the heat sink type under consideration. The quasi-complete search of defined solution domain was then performed and the different heat sink designs were compared by means of thermal performance metrics, i.e., array, space claim and mass based heat transfer coefficients. The computational fluid dynamics (CFD) calculations were repeated for the most effective heat sink designs.

**Key words:** heat transfer, design optimization, heat sink, neural network approximation, numerical modeling, thermally conductive polymer.

### 1. Introduction

Heat sinks are the most common hardware used for the heat dissipation. They are employed in microelectronic devices as well as in high power electrical components and are considered to be the simplest and the cheapest cooling solution. With constantly increasing demands for the heat dissipation the optimization of the heat sink design has become a key issue. In most cases, an improvement of the heat sink thermal performance has to be made with respect to the practical constrains like the available pressure drop, external dimensions, mass, volume or price. For many years the optimization was done basing on the analytical models or strongly simplified numerical models of the heat sinks. Nowadays, workstations with high computational power become common engineering tools and the complex computational fluid dynamics (CFD) simulations might be applied for the thermal analyses and design optimization of the heat sinks.

---

\* To whom correspondence should be addressed

## 1.1. Literature review

The heat sink design optimization was addressed in various publications (Lee, 1995; Bahadur and Bar-Cohen, 2005; Chen *et al.*, 2005). Lee (1995) presented the optimization approach which was based on an analytical simulation model for predicting thermal performance of heat sinks. The effect of various design parameters on the performance of a heat sink was illustrated. The work included also two heat sink classifications. One was based on the cooling mechanism employed to remove the heat from the heat sink and the other on the manufacturing methods and the final heat sink shape. The first categorization named passive, semi-active and active heat skins, liquid cooled cold plates and phase change systems. The other classification included stampings, extrusions, bonded or fabricated fins, castings and folded fins and referred to metallic made heat sinks. The work by Lee (1995) was mainly focused on active extruded heat sinks.

Aluminum is still the most widely used material for manufacturing of heat sinks due to its high thermal conductivity, relatively low weight and price. However, a new class of polymers characterized by high thermal conductivity has been introduced into the market recently (Coolpolymers Inc., 2012). The availability of such materials combined with the application of the injection molding process extends the flexibility of the heat sink shape. Thermal conductivity of such polymers is up to  $20 \text{ W/mK}$  which is much less than aluminum. However, lower heat conduction can be compensated by the convection and radiation from a more complex external surface, especially in natural convection heat sinks, where the main limiting factor for the heat dissipation is the heat transfer coefficient. The weight reduction is an additional advantage of a plastic heat sink as well as the unique possibility of electrically insulating properties, that is particularly important in the electronic and electrical applications.

Bahadur and Bar-Cohen (2005) presented a design and optimization methodology for the polymer staggered pin fin heat sinks. The proposed approach was dedicated to the natural convection heat sinks and was based on the application of the correlation developed by Aihara *et al.* (1990). The influence of heat sink geometric parameters like the pin fin height, pin diameter, horizontal spacing and pin fin density on the heat dissipation capabilities was discussed and the thermal performance metrics were proposed for that purpose. The overall thermal capability of a convective heat sink was represented by array Eq.(1.1), space claim Eq.(1.2) and mass based Eq.(1.3) heat transfer coefficients.

$$h_A = \frac{q_T}{LW\Theta_b}, \quad (1.1)$$

$$h_{SC} = \frac{q_T}{LWH\Theta_b}, \quad (1.2)$$

$$h_M = \frac{q_T}{V\rho_p\Theta_b}. \quad (1.3)$$

The array heat transfer coefficient is defined as the ratio of the heat sink cooling rate  $q_T$  to the area occupied by the array of pin fins and to the base plate excess temperature  $\Theta_b$ . In Eq.(1.1)  $L$  and  $W$  are the array length and width, respectively. In the space claim heat transfer coefficient the array area is extended to the volume occupied by the pin fins and  $H$  in Eq.(1.2) is the height of the pin fin. Finally, in the mass based heat transfer coefficient the heat sink cooling rate  $q_T$  is divided by the base plate excess temperature  $\Theta_b$  and by the mass of the pin fin. In Eq.(1.3)  $V$  and  $\rho$  are the pin volume and the fin material density respectively.

The methodology proposed by Bahadur and Bar-Cohen (2005) was validated and verified with the experimental measurements and CFD simulations. The obtained results revealed limitations related to the correlation proposed by Aihara *et al.* (1990), which was originally restricted to the heat sinks with fins density in a range of  $2.25\text{-}10.8 \text{ fins/cm}^2$ . For the heat sinks fulfilling this requirement the prediction of

thermal efficiency had the accuracy within  $\pm 10\%$ , while for the ones that exceeded these boundaries as much as 30% over prediction was observed.

Chen *et al.* (2005) presented a method for thermal optimization of a pin fin heat sink under multiple constraints like the available pressure drop, the space limitations and the mass restrictions. In the proposed approach: (a) statistical methods were applied for the sensitivity analysis of the design factors, (b) the design of experiments (DOE) and the response surface methodology (RSM) were used for the development of regression models of the thermal resistance and pressure drop in terms of the design factors and (c) the gradient-based numerical optimization technique was employed in the search for optimal design parameters. Thermal and hydrodynamic models of the pin fin heat sink were developed for evaluation of the thermal resistance and the pressure drop. These analytical models were validated with the use of experimental data, showing good accuracy, which was superior to the solution obtained using the commercial CFD software, Icepak (Fluent Inc., 2002).

The key concept of the approach proposed by Chen *et al.* (2005) was the application of the DOE and the RSM in the heat sink optimization. A short presentation of these statistical methods for establishing the explicit relationships between the design variables and the responses in an explored system was made by the authors and more information on this topic can be found in the related literature (Montgomery, 1997; Wu and Hamada, 2000; Myers and Montgomery, 2002). The example calculations were made for a pin fin heat sink, but the proposed optimization procedure is not limited to any particular design.

Chen *et al.* (2005) used the traditional RSM in which the second-order polynomial model – Eq.(1.4) – was applied for the approximation of the experimental results, where  $\beta_i$  represents the linear effect of design variables  $x_i$ ,  $\beta_{ii}$  represents the quadratic effect of  $x_i$ ,  $\beta_{ij}$  represents the linear-by-linear interaction between  $x_i$  and  $x_j$ , and  $\varepsilon$  is the fitting error.

$$y = \beta_0 + \sum_i \beta_i x_i + \sum_i \beta_{ii} x_{ii} + \sum_{ij} \beta_{ij} x_{ij} . \quad (1.4)$$

The statistical requirements related to the polynomial approximation require the data from strictly defined points for the model development. It means that the values of design parameters such as the fin height, the diameter of fin and their density are precisely defined. One might imagine a situation in which these requirements could not be fulfilled, e.g., due to the limitations in the heat sink manufacturability or the experimental setup. In some cases also the approximation with a single polynomial surface may not provide sufficient accuracy for the analysis of different heat sink shapes. In such circumstances, alternative approximation methods could be applied and the artificial neural networks are the example.

Beyer *et al.* (2006) presented an application of the response surface methods based on the neural networks in the field of engineering. A short presentation of the neural network concept was made by the authors and more detailed information can be found in the related literature (Hassoun, 1995; Gurney, 1997; Tadeusiewicz, 1993).

In general, neural networks with their structure and performance imitate the human brain. A neuron is a basic component of the network (Fig.1). It is capable of mapping several input signals into a single output, according to the so called activation function. The most common design of a neural network, which is called the feedforward neural network, consists of several layers which are composed of a number of neurons (Fig.2). The neurons from the same layer are not connected to one another. Instead, their outputs are used as the input signals for each neuron in the following layer. The goal of such network is processing of the input signals and changing them into one or more outputs. Such a process can be applied to the classification, approximation or optimization.

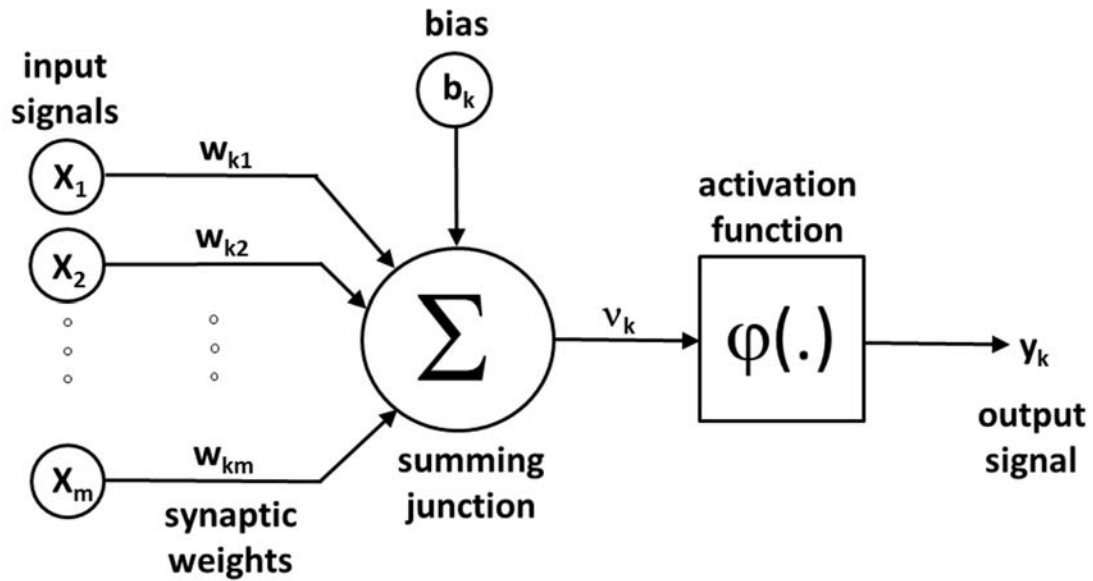


Fig.1. Structure of neuron (Beyer *et al.*, 2006).

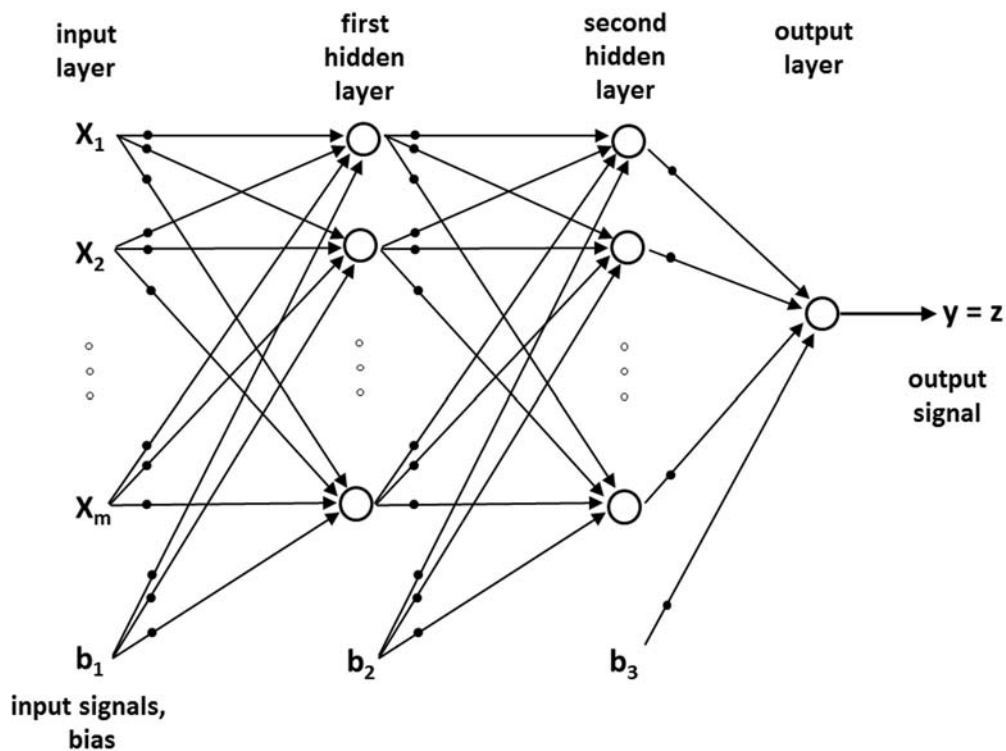


Fig.2. Structure of feedforward neural network (Beyer *et al.*, 2006).

Development of a neural network requires a training. A predefined set of input and output signals is used for evaluating weights between the neuron connections (synapses). The common approach is the utilization of two sets of predefined inputs and outputs. The first one is used for the network learning while the other for testing of its accuracy.

The training process could be considered as an optimization problem in which an error of a neural network should be minimized and the neuron weights are the independent variables. Traditionally, the neuron weights are searched with the gradient descent algorithms, e.g., the backpropagation of error. These techniques are good enough for most uses, but are susceptible to local optima. Kennedy *et al.* (2001) discuss that issue in their work and propose an alternative approach which is based on the particle swarm optimization (PSO) method.

The PSO (Kennedy *et al.*, 2001) is a stochastic optimization method with root in the numerical modeling of natural phenomena like the movement of a school of fish, flock of birds or swarm of flying insects. In that method a limited population of potential solutions (particles) is used for searching of a solution domain. During the consecutive iterations these particles are moving through the search space. The velocity and the direction of each particle is defined independently basing on: its speed in previous iteration, position of the best solution found by the particle so far and position of the best solution found by other particles. Moreover, the influence of the mentioned factors for each particle and in each moving step iteration is random. The final solution is obtained when all particles gather around one spot in the solution domain.

It is considered that the PSO, like other stochastic optimization methods, demonstrates resistance to the local optima. Additionally, it is characterized by fast convergence. Kennedy *et al.* (2001) shortly described the application of the PSO to neural network learning referring to work of Eberhart *et al.* (1996) for more details. The discussed example indicated the PSO capabilities, when 3.5 hours of training time for the traditional backpropagation method was reduced to 2.2 minutes with the PSO applied as a training algorithm.

## 1.2. Scope of investigation

This paper deals with the analysis of the thermal efficiency and the design optimization of a staggered pin fin heat sink made of a thermally conductive polymer. It is a passive heat sink according to Lee (1995) classification, thus natural convection and radiation are the main heat dissipation mechanisms.

The steps of the procedure for the analysis and optimization of selected heat sink design are as follows:

- a) selection of design parameters and their ranges
- b) performance of a limited number of experiments for selected heat sink shapes
- c) determination of a response surface by employing the neural network approximation
- d) searching of an optimal design basing on the selected heat sink performance metrics
- e) verification of “the best” design – performing experiments for the selected optimal heat sink designs.

The geometry of the heat sink is shown in Fig.3. For the purpose of analysis and optimization it is assumed that the dimensions of the base plate are fixed to  $25 \times 25 \times 3$  mm. The design parameters selected for the optimization are listed below together with their ranges:

- $N$  is number of pin fins on the base plate diagonal: 5, 7 or 9
- $d$  is diameter of the pin fin top: 1.0-3.0 mm
- $H$  is pin fin height: 20.0-40.0 mm

The selected heat sink material is CoolPoly® E5101 (Coolpolymers Inc., 2012) and its properties are:

- density: 1700 kg/m<sup>3</sup>
- specific heat: 900 J/kgK
- thermal conductivity: 20 W/mK

The heating power of 9.375 W at the base plate and the ambient temperature of 25°C were also assumed for the purpose of design optimization.

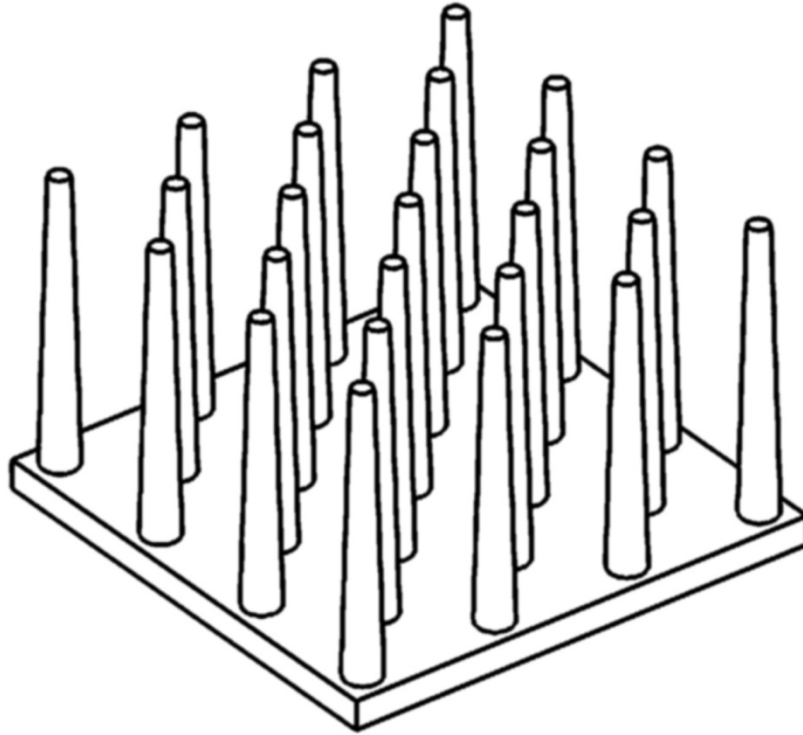


Fig.3. Heat sink design under consideration.

### 1.3. Paper structure

This paper consists of several sections. This section includes an introduction, literature review and scope of the presented work. The next one is dedicated to the numerical model of the heat sink and the CFD simulations. Experimental and simulation results are compared, allowing evaluation of the numerical model accuracy. The subsequent section presents the procedure of analysis and optimization, and each step is described with more details. The results are presented in a separate section and the influence of selected design parameters on the heat sink performance is discussed.

### 2. CFD model

The response surface from step (c) in section 1.2. is developed basing on data from a limited number of experiments. Real experiments are difficult as they would require manufacturing of several heat sinks that differ in pin fin number, diameter and height. The approach in which physical heat sinks are replaced with the analytical models is presented for example by Lee (1995), Bahadur and Bar-Cohen (2005) or Chen *et al.* (2005). In the last mentioned paper the numerical model based on the commercial CFD software Icepak (Fluent Inc., 2002) is also tested. However, when compared to experimental measurements, it provides less accurate results in comparison with the analytical model.

The uncontested advantage of numerical modeling and CFD simulations is that the conductive, convective and radiative heat transfers are directly solved and potentially any type and any shape of a heat sink could be analyzed. The increase of the computational power of workstations allows the application of more precise discretization (high density meshes) and advanced physical models, while the parallel computing shortens calculation times. That is why the analysis and optimization of the heat sink design presented in this paper is based on the numerical model and the commercial CFD software ANSYS Fluent (ANSYS, Inc., 2009; 2009a) is used for that purpose.

## 2.1. Basics of numerical model

The proposed numerical model includes the geometry of the pin fin heat sink and the representative volume of surrounding air. Mathematical models solved in the calculations have to represent all important physical phenomena like the buoyancy driven and turbulent air flow or the conductive, convective and radiative heat transfer.

In the ANSYS Fluent the mass – Eq.(2.1.) – and momentum – Eq.(2.2.) – conservation equations are solved for any flow type. Moreover, the energy conservation equation – Eq.(2.3.) – is added for the flows that involve the heat transfer. The heat transfer inside non-moving solid regions is governed by Eq.(2.4), which is a simplified form of Eq.(2.3).

$$\frac{\partial p}{\partial t} + \nabla \cdot (\rho \mathbf{v}) = S_m, \quad (2.1)$$

$$\frac{\partial}{\partial t} (\rho \mathbf{v}) + \nabla \cdot (\rho \mathbf{v} \mathbf{v}) = -\nabla p + \nabla \cdot (\bar{\boldsymbol{\tau}}) + \rho \mathbf{g} + \mathbf{F}, \quad (2.2)$$

$$\frac{\partial}{\partial t} (\rho E) + \nabla \cdot (\mathbf{v}(\rho E + p)) = \nabla \cdot \left( k_{eff} \nabla T - \sum_j h_j \mathbf{J}_j + (\boldsymbol{\tau}_{eff} \cdot \mathbf{v}) \right) + S_h, \quad (2.3)$$

$$\frac{\partial}{\partial t} (\rho h) = \nabla \cdot (k \nabla T) + S_h. \quad (2.4)$$

The set of equations is extended with the additional transport equations when the flow is turbulent. The form of these transport equations depends on the selected turbulence model and ANSYS Fluent offers a large number of choices, e.g., the Spalart-Allmaras model (Spalart and Allmaras, 1992) preferred by the authors of this paper.

The natural convection and buoyancy driven flow are solved when the air density  $\rho$  in Eqs (2.1)-(2.3) is temperature dependent and employment of the ideal gas law – Eq.(2.5.) – is one of the methods. In this work other air properties, i.e., the specific heat, the thermal conductivity and the dynamic viscosity, are also defined as temperature dependent.

$$\rho = \frac{p}{\frac{R}{M} T}. \quad (2.5)$$

The radiative heat transfer is included in the heat transfer equation – Eq.(2.3.) – by means of the heat source term  $S_h$ . It is defined by different formulas depending on the selected radiation model and among several others the so called Discrete Ordinates (DO) Radiation Model (Chui and Raithby, 1993; Raithby and Chui, 1990) is offered by the ANSYS Fluent.

Although with the proposed numerical model the time dependent analysis is possible, the analysis of the heat sink thermal performance is limited to the steady state conditions. The heating up time is irrelevant for the purpose of design optimization. In such a situation it is worth noting that removing the time from the heat transfer equation in the solid regions – Eq.(2.4) – makes the thermal conductivity  $k$  the only property of the heat sink material that has influence on the temperature distribution.

## 2.2. Numerical model validation and verification

Regardless of whether the heat sink model is numerical or analytical, its validation and verification is always required. The accuracy of the proposed numerical model is tested by comparison of the temperature values coming from experimental measurements and corresponding simulations.

The experimental stand with the pin fin heat sink made of the thermally conductive thermoplastic material CoolPoly® E5101 is shown in Fig.4. The heat sink is mounted on a copper plate, on which opposite side a thin heater was glued. Below the heater a thick layer of thermal insulating material is attached in order to force the heat flow in a direction from the heater towards the heat sink. The whole assembly of the heat sink with the copper plate, heater, and insulation layer is hung on strings.

Experimental results comprise rise of the heater temperature measured for several levels of heating power, which is controlled through settings of voltage and current at DC power supply device.

The geometry considered in the numerical model of the experimental setup is depicted in Fig.5. The existing symmetry planes allow limitation of the numerical model only to one eighth of the heat sink and go far toward reduction of calculation time.

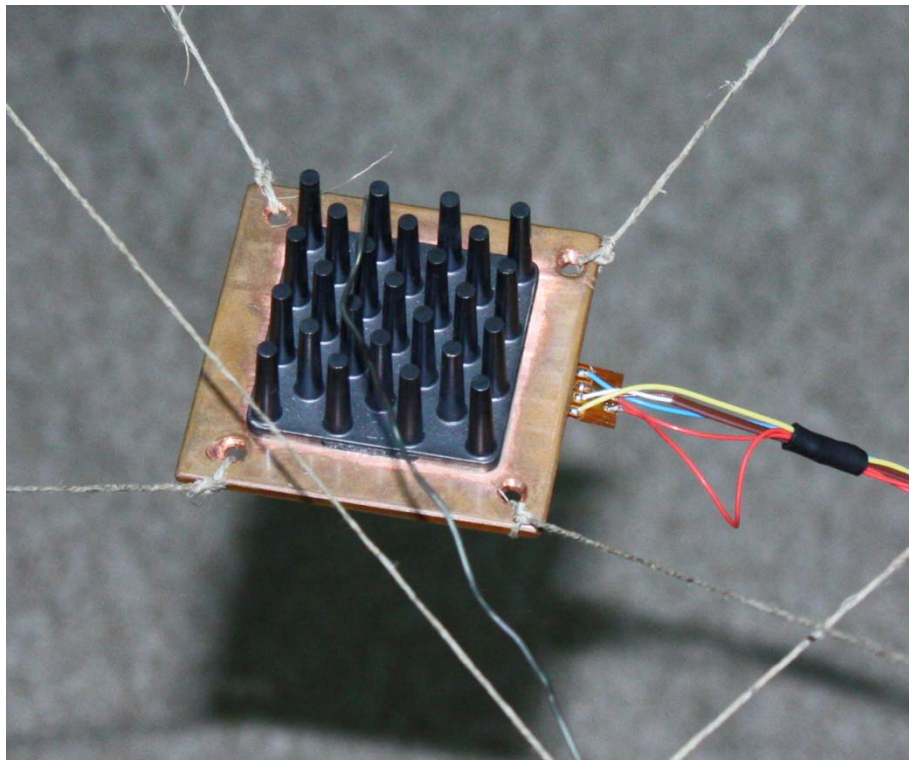


Fig.4. Heat sink used for validation and verification of numerical model.

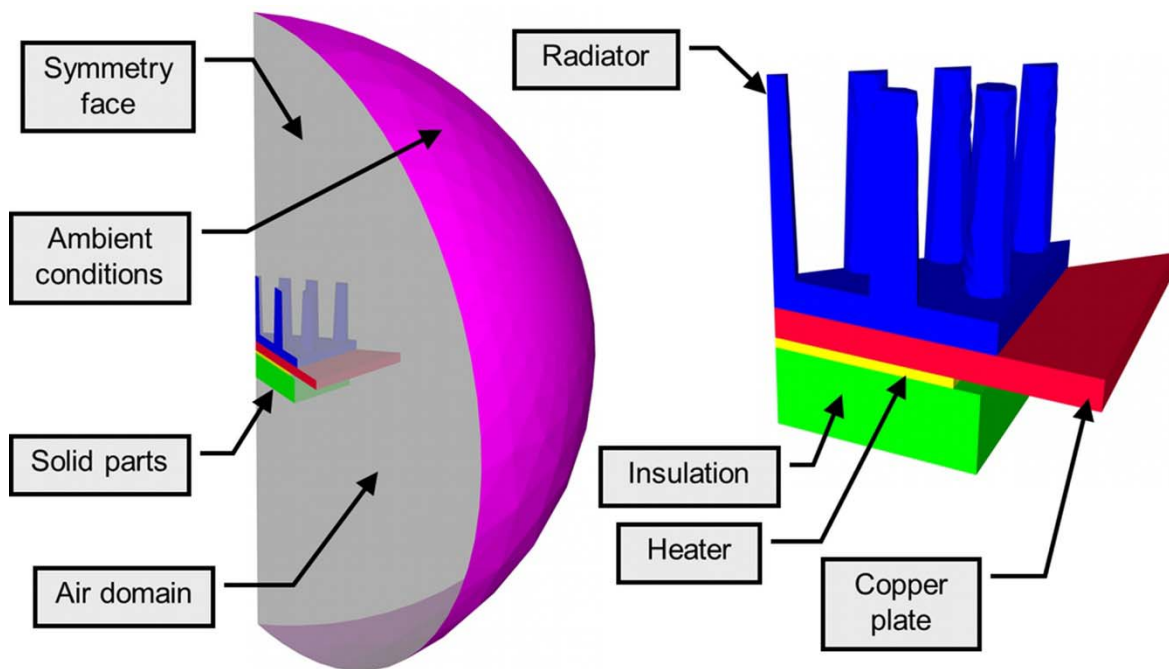


Fig.5. Numerical model geometry.

The results of the measurements and simulations are presented in Tab.1. The accuracy of the numerical model is evaluated with the absolute and the percent error. It could be noticed that the calculated temperature is always slightly higher than the measured one. The absolute error is increasing and the percent error is decreasing with the rise of the measured heater temperature. The measurement error is considered as the main reason for the high value of the percent error in the first two experiments. The typical accuracy of a T-type thermocouple is  $0.5\text{ K}$  or  $1.0\text{ K}$  depending on the sensor class. It is a significant value in comparison to the absolute error of performed measurements. Finally, it is concluded that the numerical model provides accurate results and it could be used as the replacement of real experiments.

Table 1. Results of verification of numerical heat sink model.

Exp.	Voltage	Current	Heating power	Measured rise of heater temp.	Computed rise of heater temp.	Absolute error	Percent error
	<i>V</i>	<i>A</i>	<i>W</i>	<i>K</i>	<i>K</i>	<i>K</i>	<i>%</i>
01	2.024	0.182	0.368	3.92	4.70	0.78	19.9
02	4.027	0.374	1.506	13.69	15.67	1.98	14.5
03	6.025	0.563	3.392	27.36	29.61	2.25	8.2
04	6.022	0.563	3.390	27.18	29.21	2.03	7.5
05	8.096	0.749	6.064	43.82	46.68	2.86	6.5
06	10.044	0.942	9.461	64.00	67.01	3.01	4.7

In Figs 6-8 examples of the results from computer simulations are presented including: paths of air buoyancy driven flow and temperature distribution at the heat sink surface.

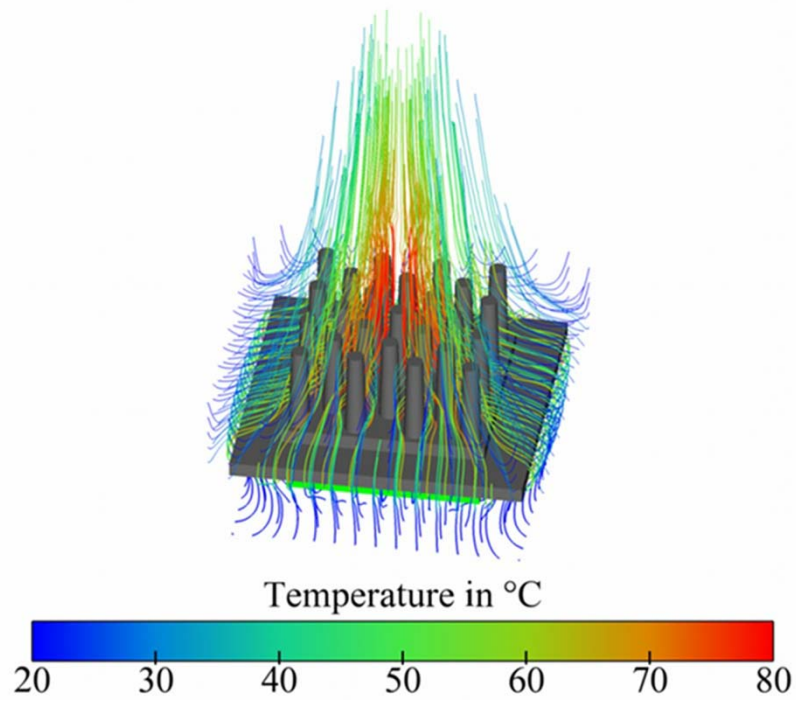


Fig.6. Natural convection flow paths colored by air temperature.

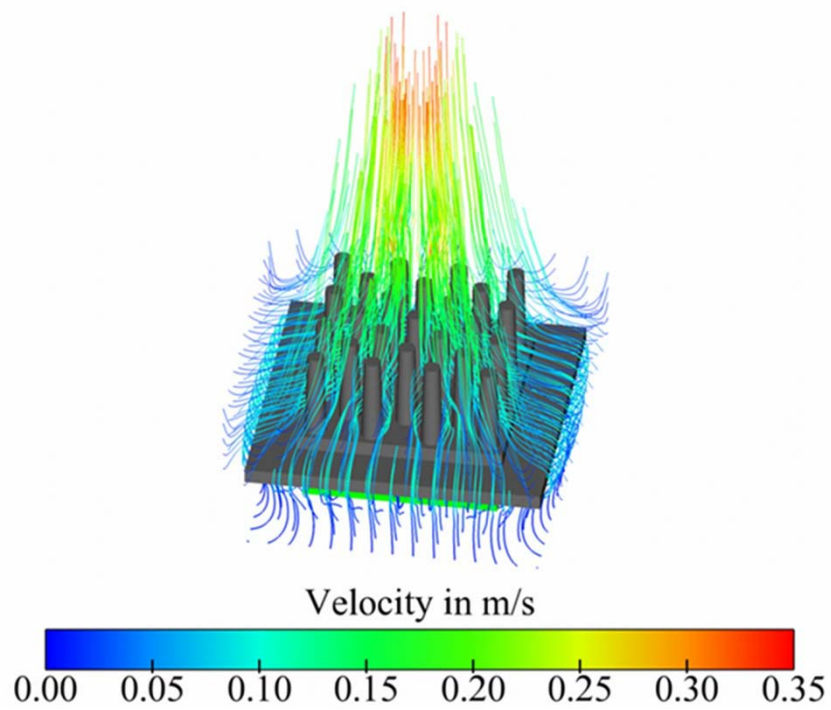


Fig.7. Natural convection flow paths colored by air velocity magnitude.

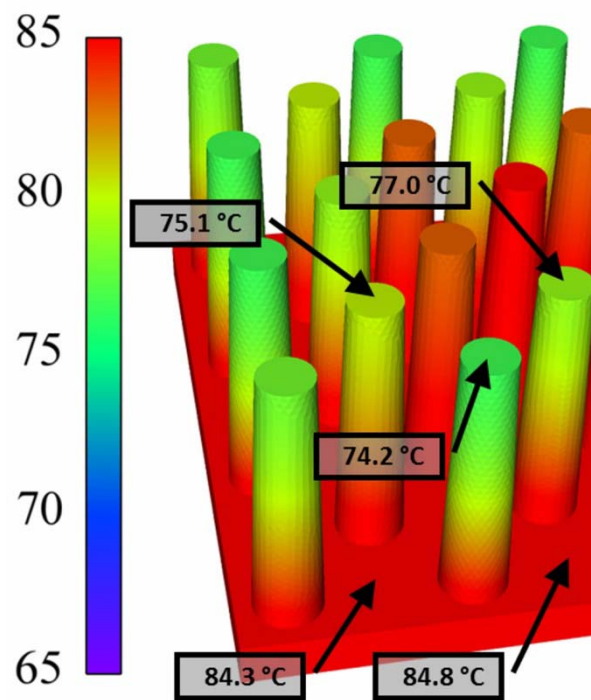


Fig.8. Temperature distribution at heat sink surface; temperatures indicated by arrows come from infrared measurements.

### 3. Heat sink analysis and optimization

The procedure proposed in section 1.2. is applied for the analysis and optimization of the heat sink design. In step (a) the design parameters and their ranges are defined. They are presented in section 1.2. In step (b) virtual experiments are performed for the fifteen chosen heat sink designs and the numerical model, as presented earlier in this paper, is used for that purpose. The analyzed heat sink designs are described in Tab.2. The values of design variables in these experiments are selected according to the central composite plan for three dimensions, known from the DOE methodology, or more precisely the face-centered central composite design as defined by Montgomery (1997). Its graphical representation is shown in Fig.9.

Table 2. Heat sink designs selected for virtual experiments.

Design parameter	Experiment 01	Experiment 02	Experiment 03	Experiment 04	Experiment 05	Experiment 06	Experiment 07	Experiment 08	Experiment 09	Experiment 10	Experiment 11	Experiment 12	Experiment 13	Experiment 14	Experiment 15
<b>N</b>	7	5	5	5	5	9	9	9	9	7	7	7	7	9	7
<b>d</b>	2.0	1.0	3.0	1.0	3.0	1.0	3.0	1.0	3.0	1.0	3.0	2.0	2.0	2.0	2.0
<b>H</b>	30.0	20.0	20.0	40.0	40.0	20.0	20.0	40.0	40.0	30.0	30.0	40.0	20.0	30.0	30.0

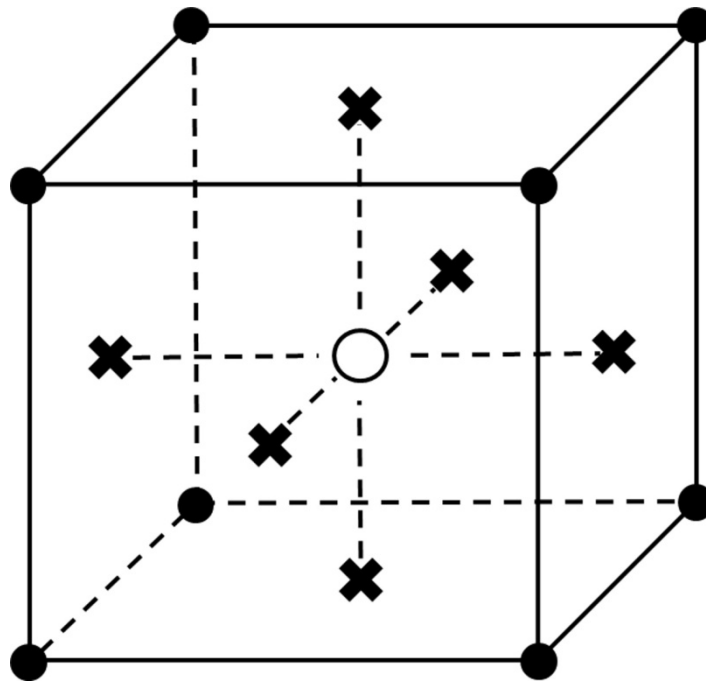


Fig.9. Face-centered central composite design plan of experiments.

The experiment 01 is called center point and in Fig.9. it is displayed as a circle. In that experiment the medium value of each heat sink design parameter is selected. The next eight experiments are called cube or corner points and in Fig.9. are represented by dots. In these experiments the extreme values of each design parameter are combined, similar as it is in the full factorial plan at two levels. The last six experiments, shown in Fig.9. as crosses, are called axial or star points. The chosen values of design parameters are combinations of medium and extreme numbers from available ranges.

The experimental results are shown in Tab.3. The measured value is the base plate temperature rise. It is computed as the difference between the mean temperature of the heat sink bottom surface and the ambient temperature which is 25 °C.

In step (c) the response surface is developed and the neural network approximation is used for that purpose. The input variables are the number of pin fins on the base plate diagonal, the diameter of the pin fin at its top and the pin fin height. The output is the temperature rise of the base plate.

The neural network is trained with the use of the results from the first nine experiments and tested with the results from the remaining six experiments. It is trained by application of the particle swarm optimization method. Two hidden layers with twelve neurons in each layer provide very good accuracy of the network output. The neural network error shown in Tab.3. is calculated with Eq.(3.1), where  $\Theta_b$  is the heat sink base temperature rise, while  $CFD$  and  $NN$  stand for the simulation and the neural network results, respectively. It can be noticed that the error of the learning set is below 0.05% and the error of the testing set is below 2.0%.

$$Error = \frac{|\Theta_b^{NN} - \Theta_b^{CFD}|}{\Theta_b^{CFD}} \cdot 100\% . \quad (3.1)$$

Table 3. Results of experiments and comparison to neural network approximation.

Experiment	$N$ (-)	$d$ (mm)	$H$ (mm)	$\Theta_b^{CFD}$ (K)	$\Theta_b^{NN}$ (K)	Error (%)
01	7	2.0	30.0	70.68	70.71	0.04
02	5	1.0	20.0	114.64	114.64	0.00
03	5	3.0	20.0	93.67	93.65	0.02
04	5	1.0	40.0	95.87	95.87	0.00
05	5	3.0	40.0	73.28	73.28	0.00
06	9	1.0	20.0	84.56	84.56	0.00
07	9	3.0	20.0	63.74	63.74	0.01
08	9	1.0	40.0	61.44	61.42	0.02
09	9	3.0	40.0	48.99	48.99	0.00
10	7	1.0	30.0	85.03	83.99	1.23
11	7	3.0	30.0	61.68	62.80	1.81
12	7	2.0	40.0	62.17	63.18	1.63
13	7	2.0	20.0	83.23	83.43	0.24
14	9	2.0	30.0	58.96	59.85	1.51
15	5	2.0	30.0	91.80	91.41	0.42

In step (d) the solution domain is explored and the optimal heat sink design is looked for. The neural network developed in the previous step gives an immediate response to the input signals and the computing of the base plate temperature rise for the large number of heat sink designs is possible. That is why the quasi-complete search of the solution domain is performed, instead of the application of some kind of optimization method, e.g., gradient descent, genetic algorithm. The quasi-complete search is a full combination of the following design parameters:

- number of pin fins on the base plate diagonal  $N$  equals 5, 7 or 9 (three levels)
- top diameter of pin fin  $d$  equals: 1.0, 1.2, ..., 3.0 mm (eleven levels)
- pin fin height  $H$  equals: 20.0, 22.5, ..., 40.0 mm (nine levels),

which results in 297 cases. These different designs are compared using the temperature rise of the base plate as well as the array, the space claim and the mass based heat transfer coefficients – Eqs (1.1)-(1.3) respectively. In Figs 10-13 the results obtained are illustrated and for the chart clarity only three pin fin diameters are considered.

The temperature rise of the heat sink base plate (Fig.10.), is directly correlated with selected heat sink design parameters. That temperature is decreased by a higher value of any of those parameters. It is also worth mentioning that the same temperature rise, e.g., 80.0 K, could be achieved with the heat sinks having different designs, i.e., characterized by a different number of pin fins, fin height and fin diameter.

In Fig.11 the array heat transfer coefficient is shown. According to the assumptions the same heat is dissipated by all heat sinks and the size of the base plate is also constant, thus the array coefficient depends only on the temperature rise of the base plate. It is quite obvious that for heat sink having 9 pin fins on the base plate diagonal, 3.0 mm pin fin diameter and 40.0 mm pin fin height the surface for a heat dissipation is the largest and thus the lowest base plate temperature is obtained and the array heat transfer coefficient has its maximum.

In Fig.12 the results of the space claim heat transfer coefficient are depicted. Having in mind the same assumptions as mentioned above, in this case the heat sink performance metrics is influenced by two

variables, i.e., the pin fin height and the temperature rise of the base plate. It is interesting to notice that if the number of pin fins and their diameter are fixed the space claim heat transfer coefficient is decreasing with the growth of the pin fin height. Although longer fins result in lower base plate temperature, at the same time more space is occupied by the heat sink. Thus, according to the space claim heat transfer coefficient the best heat sink design consists of a large number of short and thick pin fins, i.e., 9 pin fins on the base plate diagonal with the diameter of 3.0 mm and height of 20.0 mm.

In Fig.13 the mass based heat transfer coefficient is presented. These results are the most difficult to analyze because all three design parameters have a direct influence on the heat sink performance metrics. In general, a small pin fin thickness seems to be the best choice, but that design parameter is less important in heat sinks having also a small number of short pin fins. It could also be noticed that increasing the number of pin fins on the base plate diagonal increases also the influence of the remaining design parameters on heat sink efficiency. Finally, design parameters of the best heat sink are: 9 pin fins on the base plate diagonal, the pin fin diameter of 1.0 mm and the pin fin height of 25.0 mm. It is worth mentioning that the best designs resulting from the array and the space claim heat transfer coefficients are placed at the edge of the solution domain, while the one related to the mass based heat transfer coefficient is positioned inside.

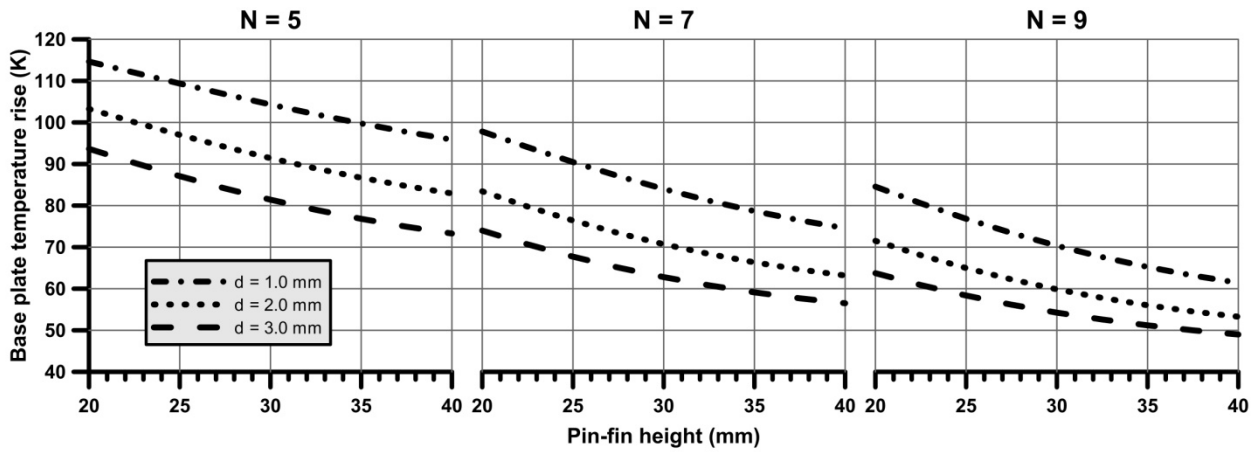


Fig.10. Temperature rise of heat sink base plate.

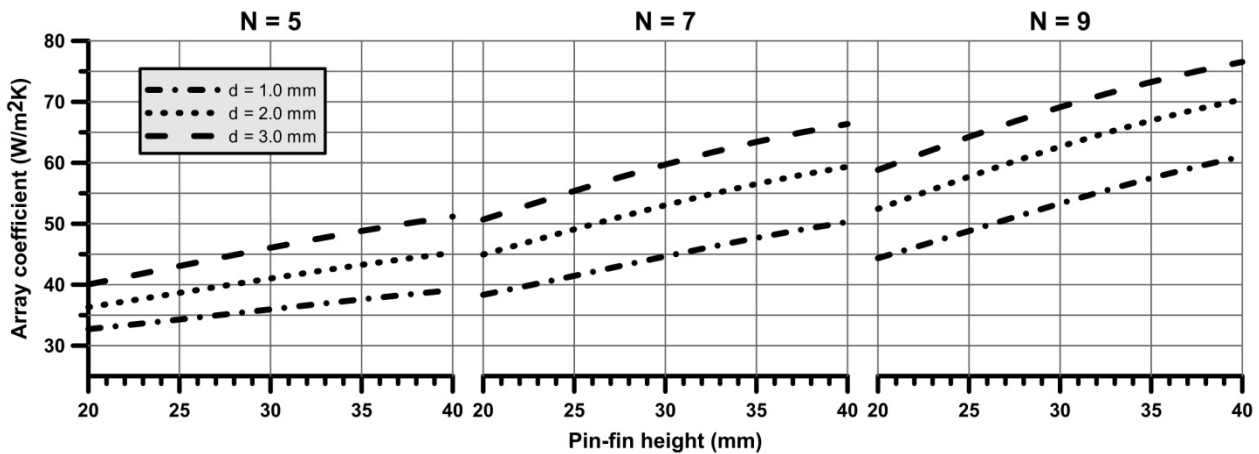


Fig.11. Array heat transfer coefficient.

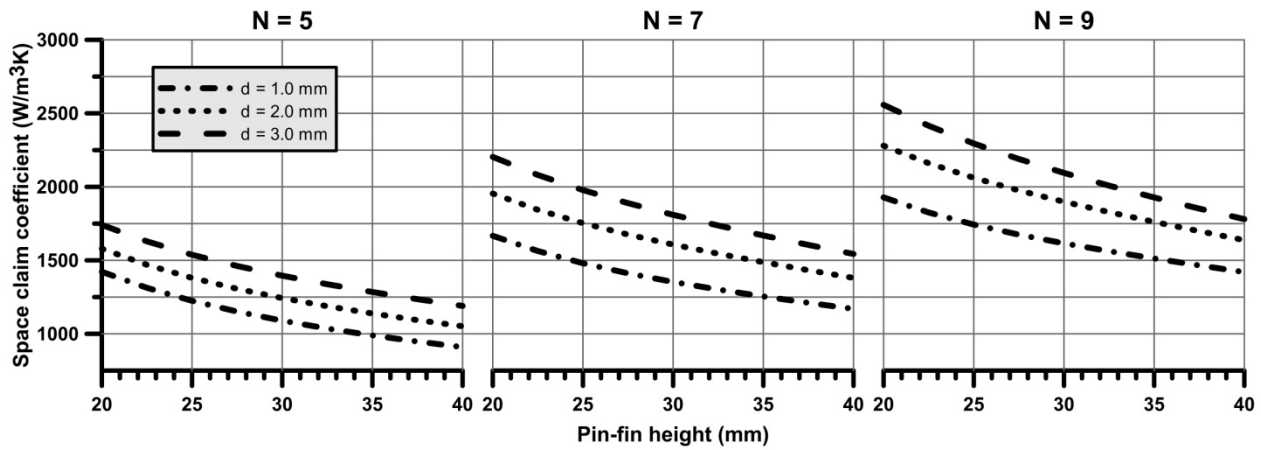


Fig.12. Space claim heat transfer coefficient.

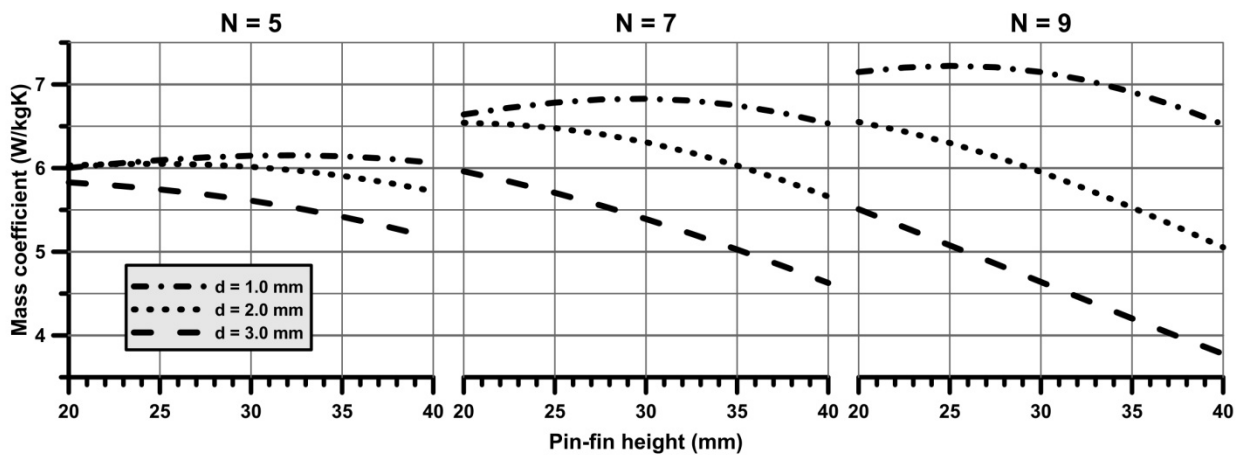


Fig.13. Mass based heat transfer coefficient.

In step (e), the best solutions are verified. It is required because the results from the analysis and optimization of the heat sink design are based on the heat sink model in the form of an artificial neural network and they contain the approximation error. The verification is done through creation of numerical models of the best heat sink designs and comparison of the base plate temperature rise calculated with the neural network and that obtained in CFD simulations.

Such a comparison for the optimum design resulting from the array and the space claim heat transfer coefficients is already made in Tab.3., as all these designs were included in the neural network training set – experiment 09 and experiment 07, respectively. The CFD simulations of the best design for the mass based heat transfer coefficient were made separately and the obtained error was equal to 0.03%.

#### 4. Summary

The influence of selected design parameters on the cooling efficiency of a polymer made pin fin heat sink is analyzed. The following design parameters are considered: the pin fin top diameter, the pin fin height and the number of pin fins. The optimum design is searched regarding various metrics of the heat sink cooling efficiency and a neural network model of the heat sink thermal performance is utilized for that purpose. The neural network model is developed basing on the results from a limited number of experiments

in which selected designs of the heat sink are tested. The experiments are performed by applying a validated and verified numerical model of the heat sink, thus manufacturing of the real specimens is not required.

## Nomenclature

$d$	– top diameter of pin fin, [m]
$E$	– total energy, [J]
$F$	– force, [N]
$g$	– gravitational acceleration, [ $m/s^2$ ]
$H$	– height of the pin, [m]
$h$	– heat transfer coefficient, [ $W/m^2K$ ]
$h$	– enthalpy, [J/kg]
$J$	– mass flux or diffusion flux, [ $kg/m^2s$ ]
$k$	– thermal conductivity, [ $W/mK$ ]
$L$	– length of array, [m]
$M$	– molecular weight, [ $kg/kgmol$ ]
$N$	– number of pins on base diagonal, [-]
$p$	– pressure, [Pa]
$q$	– heat sink cooling rate, [ $W$ ]
$R$	– gas law constant, $8.31447 \cdot 10^3$ [ $J/kgmolK$ ]
$S$	– mass or energy source, [ $kg/m^3s$ ] or [ $J/kgmolK$ ]
$T$	– temperature, [K]
$t$	– time, [s]
$v$	– velocity, [ $m/s$ ]
$V$	– volume, [ $m^3$ ]
$W$	– width of the pin array, [m]
$\Theta$	– excess temperature, [K]
$\rho$	– density, [ $kg/m^3$ ]
$\bar{\tau}$	– stress tensor, [Pa]

## Subscripts

$A$	– array
$b$	– base of fin array
$eff$	– effective
$M$	– mass
$p$	– pin fin
$SC$	– space claim
$T$	– total

## References

- Aihara T., Maruyama S. and Kobayakawa S. (1990): *Free convective/radiative heat transfer from pin-fin arrays with a vertical base plate (general representation of heat transfer performance)*. – International Journal Heat Mass Transfer, vol.33, No.6, pp.1223-1232.
- ANSYS. Inc. (2009): *ANSYS FLUENT 12.0 Theory Guide*.
- ANSYS. Inc. (2009a): *ANSYS FLUENT 12.0 User's Guide*.
- Bahadur R. and Bar-Cohen A. (2005): *Thermal design and optimization of natural convection polymer pin fin heat sink*. – IEEE Transactions on Components Packing and Manufacturing Technology, vol.28, No.2, pp.238-246.
- Beyer W., Liebscher M., Beer M. and Graf W. (2006): *Neural Network Based Response Surface Methods – a Comparative Study*. –LS-DYNA Anwenderforum, Ulm.

- Chen H-T., Chen P-L, Horng J-T. and Hung Y-H (2005): *Design optimization for pin-fin heat sinks*. – Journal of Electronic Packaging, vol.127, pp.397-406.
- Chui E.H. and Raithby G.D. (1993): *Computation of Radiant Heat Transfer on a Non-Orthogonal Mesh Using the Finite-Volume Method*. – Numerical Heat Transfer, Part B 23:269-288.
- Coolpolymers Inc. (2012): *www.coolpolymers.com* – Warwick, RI, USA.
- Eberhart R.C., Simpson P.K. and Dobbings R.W. (1996): *Computational Intelligence PC Tools*. – Boston: Academic Press.
- Fluent Inc. (2002): *Icepak 4: Advanced Thermal Modeling Software for Electronic Design*. – Lebanon, NH, USA.
- Gurney K. (1997): *An Introduction to Neural Networks*. – CRC Press.
- Hassoun M.H. (1995): *Fundamentals of Artificial Neural Networks*. – The MIT Press.
- Jeff Wu C.F. and Hamada. M. (2000): *Experiments – Planning. Analysis and Parameter Design Optimization*. – John Wiley & Sons.
- Kennedy J., Eberhart R.C. and Shi Y. (2001): *Swarm Intelligence*. – Morgan Kaufmann.
- Lee S. (1995): *Optimum Design and Selection of Heat Sinks*. – IEEE Transactions on Components Packing and Manufacturing Technology, vol.18, No.4, pp.812-817.
- Montgomery D.C. (1997): *Design and Analysis of Experiments*. – 4th edition, John Wiley & Sons.
- Myers G.N. and Montgomery D.C. (2002): *Response Surface Methodology, 2nd edition*. – John Wiley & Sons.
- Raithby G.D. and Chui E.H. (1990): *A Finite-Volume Method for Predicting a Radiant Heat Transfer in Enclosures with Participating Media*. – J. Heat Transfer, 112:415-423.
- Spalart P. and Allmaras S. (1992): *A one-equation turbulence model for aerodynamic flows*. – Technical Report AIAA-92-0439, American Institute of Aeronautics and Astronautics.
- Tadeusiewicz R. (1993): *Sieci Neuronowe (Neural Networks)*. – Academic Publishing House.

Received: November 6, 2012

Revised: January 8, 2013